Journal of Applied Analysis and Computation
Volume 12, Number 2, April 2022, 850–861
Website:http://www.jaac-online.com
DOI:10.11948/20210479

STUDIES ON PULL-IN INSTABILITY OF AN ELECTROSTATIC MEMS ACTUATOR: DYNAMICAL SYSTEM APPROACH

Xiangshuo Liu[1], Lijun Zhang[1,2,†] and Mingji Zhang[3]

Abstract The pull-in instability of an electrostatic microstructures is a common undesirable phenomenon which implies the loss of reliability of micro-electromechanical systems. It is important to better understand its mechanism and then to reduce the occurrence of such phenomenon. Our work is devoted to analyzing the pull-in instability of a typical electrostatic micro-electro-mechanical-system actuators with edge effects. The pull-in phenomenon and the dynamic threshold are examined via dynamical system approach and the qualitative theory of differential equations. Nonlinear interplays between the voltage and the initial positions are characterized, from which critical voltage values are identified. Those critical voltages play crucial roles in our analysis. Effects from other system parameters are also examined numerically. It turns out that most of the parameters involved in the MEMS oscillator have corresponding threshold values, beyond which the pull-in instability occurs.

Keywords Parallel-plate, pull-in instability, MEMS actuators, periodic solutions, dynamical system approach.

MSC(2010) 34C40, 34C60, 35B32, 70K42, 70K50.

1. Introduction

Micro-electro-mechanical-systems (MEMS) are an electromechanical integrated system, and its feature size of components and the actuating range are of the microscale. Differently from traditional mechanical processing, the manufacturing of MEMS device makes use of the semiconductor production process, which can be compatible with an integrated circuit, and includes surface micromachining and bulk miromachining. Thanks to the increasingly mature process technology, many sophisticated micro structural and functional modules are currently available. Correspondingly, much greater optimized performance of the device has been developed. In particular, we would like to point out that the great advantage of electrostatic-driven MEMS devices lies in its rapid response, lower power consumption, and integrated circuit standard process compatibility (see [3, 7, 11, 19, 21] for more detailed details).

†The corresponding author. Email address:li-jun0608@163.com(L. Zhang)
[1]College of Mathematics and Systems Science, Shandong University of Science and Technology, 266510 Qingdao, China
[2]International Institute for Symmetry Analysis and Mathematical Modelling, Department of Mathematical Sciences, North-West University, Mafikeng Campus, Mmabatho, South Africa
[3]Department of Mathematics, New Mexico Institution of Mining and Technology, Socorro, NM 87801, USA

Because of its simplicity of design and process, as well as convenience of integration with the integrated circuit processes to form a single-chip system, very often, the electrostatic principle is employed in sensing of MEMS or drive modules [14,15]. MEMS consists of a stationary part and a movable part connected with a voltage source. When a voltage is applied, the movable part is deformed towards the stationary position due to the attractive forces. When the voltage between the two plates reaches a threshold value, the system is in a critical equilibrium position. This position is called pull-in point, and the corresponding voltage is named as pull-in voltage. If the voltage exceeds its threshold value, the movable part touches the fixed base (stationary part), and the microstructure is kept away from the output it needs. This phenomenon is known as pull-in instability where the moving structure snaps to the actuation electrode, which is one of the most important nonlinear phenomena in electrostatic MEMS. It depends on different parameters of the forces that are used for actuating and deduction in the MEMS. In other words, a microstructure actuated electrically performs in order if the applied voltage is less than or equal to the pull-in threshold voltage, and pull-in instability occurs beyond that threshold value. Younis [24] provided a universal definition that dynamical pull-in was the collapse of the elastic structure toward the substrate induced by the combined actuation of kinetic and potential energies. Elata and Bamberger [4] and Sedighi etc [20] also agreed that dynamical pull-in belongs to the escape from the potential well of the micro-electromechanical systems. The authors in [10] studied pull-in dynamics of overdamped microbeams. He et al. introduced two numerical methods to find the approximate value of the pull-in voltage of a MEMS in [6]. Some studies [1,2,5,16,18,22] have addressed the pull-in phenomenon and presented some tools to predict its location to enable designers to avoid it.

The typical and widely used electrostatic MEMS actuators are always considered as dynamical models [9, 12, 23]. A governing equation in the form

$$m\ddot{x} + kx = F_e, \tag{1.1}$$

is applied in [24] to model the parallel-plate capacitor in a spring-mass system (see Fig. 1). Here m is the mass of the moving plate, k is the stiffness of the spring, F_e given by

$$F_e = -\frac{d}{dx}(\frac{1}{2}CV^2), \tag{1.2}$$

represents the electrostatic force, where C is capacitance and V is the direct current voltage which pulls the flexible plate towards a distance x. According to the model for the capacitance established by Love [17], when the side length of the plate w is greater than the gap between the plates d, Nemirovsky [13] approximates the effect of the fringing field capacitance on the total capacitance of a square parallel-plate actuator

$$C = \epsilon\omega\left(\frac{\omega}{d-x} + \frac{2}{\pi} + \frac{2}{\pi}\ln\big(\frac{2\pi\omega}{d-x}\big)\right), \tag{1.3}$$

where ϵ is the dielectric constant of air. Therefore, the model Eq. (1.1) becomes

$$m\ddot{x} + kx = \frac{\pi\epsilon w^2V^2 + 2\epsilon wV^2(d-x)}{2\pi(d-x)^2}, \tag{1.4}$$

which is a second-order differential equation with singularity at $x = d$.

Qualitative and bifurcation analysis theorem of differential equations is a very effective approach to study the solutions of second-order differential equations with parameters, which has been well applied in the study of traveling wave solutions of nonlinear wave equations [8,25]. In this work, we will analyze the equation (1.4) via dynamical system approach. Mathematical analysis shows that there is a unique pull-in voltage for different parameters involved in the system. Particularly, the interplays between the pull-in voltage and the parameters is characterized, and the corresponding pull-in point of the system is identified. Different types of boundary conditions are also considered, and their effects will be explored on the vibrational behavior of MEMS.

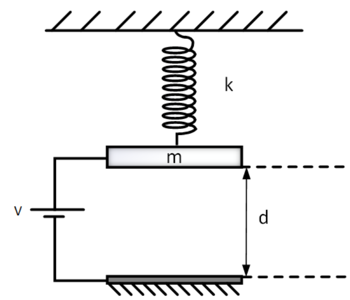

Figure 1. A single-degree-of-freedom model of a parallel-plate capacitor in a spring-mass system

The paper is organized as follows. In Section 2, we employ the dynamical system approach to analyze an electrostatic MEMS model with edge effect from the capacitor under the parallel-plate assumption. In Section 3, we discuss the pull-in instability of the electrostatic MEMS actuator from the point of more physical view. Effects from different system parameters are also studied numerically, while Section 5 provides some concluding remarks.

2. Model analysis via dynamical system approach

In our following analysis, we rescale d as $d = 1$ and introduce $A = \frac{\epsilon w^2}{2m}$, $B = \frac{\epsilon w}{\pi m}$ and $\beta = \frac{k}{m}$, then we have $A > 0$, $B > 0$ and $\beta > 0$ and the equation (1.4) becomes

$$\ddot{x} + \beta x = \frac{A}{(1-x)^2}V^2 + \frac{B}{1-x}V^2. \tag{2.1}$$

Let $\dot{x} = y$, then the equation (2.1) is equivalent to the following equations

$$\frac{dx}{dt} = y, \quad \frac{dy}{dt} = \frac{A}{(1-x)^2}V^2 + \frac{B}{1-x}V^2 - \beta x, \tag{2.2}$$

which is a Hamiltonian system. For convenience, we make a further rescaling $dt = (1-x)^2 d\tau$ when $1 - x \neq 0$, and the system (2.2) becomes

$$\frac{dx}{d\tau} = y(1-x)^2, \quad \frac{dy}{d\tau} = -\beta x(1-x)^2 + B(1-x)V^2 + AV^2. \tag{2.3}$$

The system (2.3) is an integrable system with the first integral given by

$$H(x,y) = \frac{1}{2}y^2 + \frac{\beta}{2}x^2 - \frac{A}{1-x}V^2 + BV^2 \ln|1-x|. \tag{2.4}$$

We comment that the system (2.3) has the same topological phase portraits as that of the system (2.2) except for the singular line $x = 1$.

For convenience, we introduce

$$g(x) = -\beta x(1-x)^2 + B(1-x)V^2 + AV^2, \tag{2.5}$$

and then we have

$$g'(x) = -3\beta x^2 + 4\beta x - \beta - BV^2. \tag{2.6}$$

Obviously, a point $(x^*, 0)$ is an equilibrium of the system (2.3) if $g(x^*) = 0$. However, the roots of function $g(x)$ are parameterised by β, A, B and V. To consider the effect of V, we will study it in the following two cases.

Case (1). $0 < V < \sqrt{\frac{\beta}{3B}}$

For this case, $g'(x) = 0$ has two roots $x_\pm = \frac{2}{3} \pm \frac{1}{3}\sqrt{1 - \frac{3B}{\beta}V^2}$. Let

$$h_\pm(V) = g(x_\pm) = -\beta x_\pm(1-x_\pm)^2 + B(1-x_\pm)V^2 + AV^2.$$

It follows that the function $g(x)$ is decreasing on $(-\infty, x_-)$ and reaches its local minimum value $h_-(V)$ at $x = x_-$; it is increasing on (x_-, x_+) and reaches its local maximum value $h_+(V)$ at $x = x_+$; and it is decreasing on (x_+, ∞). It is easy to see from the formulas of $x_\pm$ that $\frac{1}{3} < x_- < \frac{2}{3} < x_+ < 1$ and $g(1) = AV^2 > 0$, so one has $h_+(V) > 0$. Taking into account the limits $\lim_{x\to\pm\infty} g(x) = \mp\infty$, one has

(i) if $h_-(V) < 0$, $g(x)$ has three real roots, say x_1, x_2 and x_3, and then $0 < x_1 < x_- < x_2 < x_+ < 1 < x_3$.

(ii) if $h_-(V) = 0$, $g(x)$ has three real roots, a root $x = x_-$ of multiplicity 2 and a root $x_3 > 1$.

(iii) if $h_-(V) > 0$, $g(x)$ has only one real roots $x_3 > 1$.

Direct computation gives

$$h'_-(V) = \frac{2}{3}BV\left(1 + \sqrt{1 - \frac{3B}{\beta}V^2}\right) + 2AV.$$

Clearly, $h'_-(V) > 0$, that implies that $h_-(V)$ is increasing in V on $(0, \sqrt{\frac{\beta}{3B}})$. Since $h_-(0) = -\frac{4\beta}{27} < 0$ and $h_-(\sqrt{\frac{\beta}{3B}}) = \frac{1}{27}\beta + AV^2 > 0$, there is a unique $V^* \in (0, \sqrt{\frac{\beta}{3B}})$ such that

$$h_-(V^*) = AV^{*2} + \frac{BV^{*2}}{3}(1+N) - \frac{\beta}{27}(2-N)(1+N)^2 = 0, \tag{2.7}$$

where $N = \sqrt{1 - \frac{2B}{\beta}V^{*2}}$. It results that $h_-(V) > 0$ for $\frac{\beta}{3B} > V > V^*$ while $h_-(V) < 0$ for $0 < V < V^*$.

Case (2). $V \geq \sqrt{\frac{\beta}{3B}}$

Clearly, $g'(x) \leq 0$ and thus $g(x)$ is decreasing on the real line. Note that $g(1) > 0$ and $\lim_{x\to+\infty} g(x) = -\infty$, which indicate that $g(x)$ has unique root in $(1, +\infty)$.

Combining the analysis above, the following result can be established directly.

Lemma 2.1. *For $g(x)$, one has*

(i) *for $V > V^*$, it has a unique root in $(1, +\infty)$;*

(ii) *for $V = V^*$, it has three roots x_1, x_2 and x_3 such that $x_1 = x_2 = x_- < 1 < x_3$;*

(iii) *for $0 < V < V^*$, it has three roots x_1, x_2 and x_3 such that $0 < x_1 < x_2 < 1 < x_3$.*

Let $M(x^*, 0)$ be the coefficient matrix of the linearized system of (2.3) at an equilibrium point $(x^*, 0)$, then, one has

$$M(x^*, 0) = \begin{pmatrix} 0 & (1 - x^*)^2 \\ g'(x^*) & 0 \end{pmatrix},$$

from which $\mathrm{Tr}(M(x^*, 0)) = 0$ and $\det(M(x^*, 0)) = -(1 - x^*)^2 g'(x^*)$, where $g(x)$ is defined in (2.5).

By the theory of dynamical systems, it is well-known that for an equilibrium point of a planar integrable system, if $\det(M(x^*, 0)) < 0$, it is a saddle point; if $\det(M(x^*, 0)) > 0$ and $\mathrm{Tr}(M(x^*, 0)) = 0$, it is a center; and if $\det(M(x^*, 0)) = 0$, and the Poincare index of the equilibrium point is 0, then it is a cusp. Together with Lemma 2.1 and the discussion above, the following result can be established.

Lemma 2.2. *For the system (2.3), one has*

(i) *For $V \geq V^*$, it has a center around which there is a family of periodic orbits to the right-hand side of the singular line $x = 1$; However, every orbit to the left-hand side of the singular line approaches the singular line. In particular, for $V = V^*$, it has a cusp on the left-hand side of the singular line (see Fig. 2 (a) and (b)).*

(ii) *For $0 < V < V^*$, it has a saddle and two centers. There is a homoclinic orbit to the saddle on the left-hand side of the straight line $x = 1$ which is the boundary trajectory of a family of periodic orbits surrounding one center; There is a family of periodic orbits around the center on the right-hand side of the singular line $x = 1$. (see Fig. 2 (c)).*

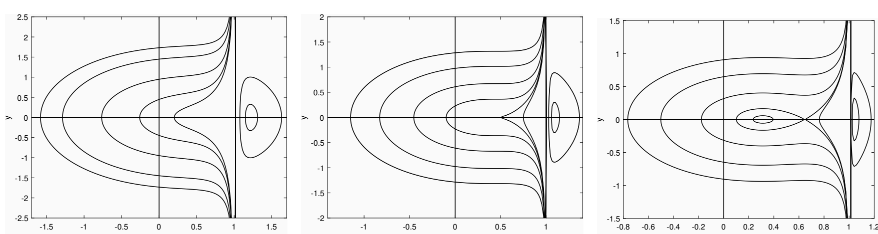

(a) $V > V^*$ (b) $V = V^*$ (c) $0 < V < V^*$

Figure 2. Phase portraits of system (2.3)

We point out that each orbit of the system (2.3) parameterized by $(x(t), y(t))$ determines a unique solution of the equation (2.1) $x = x(t)$ which is the one that we attempt to study. In particular, a periodic orbit determines a periodic solution and a homoclinic orbit corresponds to a solution approaching a finite number as time goes to infinity. However, along the orbit approaching the singular line $x = 1$, $y(t) = x'(t)$ goes to infinity, hence $x(t)$ reaches 1 in finite time, that is, the orbit approaching the singular line corresponds to a solution of the equation (2.1) $x = x(t)$ reaching 1 in finite time which is called a break solution. For instance, the orbits shown in Fig. 2 which approach the singular line all correspond break solutions of the equation (2.1). Hence, for $V \geq V^*$, all orbits to the left-hand side of the singular line correspond to break solutions except for the equilibrium point for $V = V^*$; nevertheless, for $0 < V < V^*$, the orbits outside homoclinic orbit correspond to break solutions.

For a given MEMS, it is supposed to be modeled by the equation (2.1) with initial values which are always given by the initial position of the movable plate, say $x(0) = x_0$ and $x'(0) = 0$. Therefore, we now investigate the solution of the initial value problem (IVP): the equation (2.1) and the initial values $x(0) = x_0$ and $x'(0) = 0$, which corresponds to the orbit of the system (2.3) passing through the pint $(x_0, 0)$. Therefore, one can investigate the solutions by examining the orbits passing through the point $(x_0, 0)$. Taking into account the physical background, we will not consider the case when $x_0 \geq 1$.

Lemma 2.3. *For the equation* (1.4) *subject to the initial values* $x(0) = x_0$ $(x_0 < 1)$ *and* $x'(0) = 0$, *one has*

(i) *For* $V > V^*$, *independent of the initial conditions, it has a break solution.*

(ii) *For* $V = V^*$, *it has a break solution provided that* $x_0 \neq x_-$, *however, it has a constant solution* $x = x_0$ *if* $x_0 = \frac{2}{3} - \frac{1}{3}\sqrt{1 - \frac{3B}{\beta} {V^*}^2}$.

(iii) *For* $0 < V < V^*$, *assuming that the homoclinic orbit intersects with* $y = 0$ *at* $(x_t, 0)$, *then* $x_t < x_2$ *is determined implicitly by*

$$\frac{1}{2}\beta(x_2^2 - x_t^2) + AV^2\left(\frac{1}{1 - x_t} - \frac{1}{1 - x_2}\right) + BV^2 \ln\left(\frac{1 - x_2}{1 - x_t}\right) = 0. \qquad (2.8)$$

For the equation (1.4), *one has*

(iii1) *when* $x_0 = x_c$ *or* $x_0 = x_2$, *it has a constant solution.*

(iii2) *when* $x_0 > x_2$ *or* $x_0 < x_t$, *it has a break solution.*

(iii3) *when* $x_t < x_0 < x_2$, *it has a periodic solution.*

Proof. The statements (i) and (ii) are derived directly from the first statement in Lemma 2.2.

For $0 < V < V^*$, since the point $(x_t, 0)$ is on the homoclinic orbit to the saddle $(x_2, 0)$, we have $H(x_t, 0) = H(x_2, 0)$. It follows directly from the equation (2.4) that x_t is determined implicitly by (2.8). The other statements follow directly form the second statement in Lemma 2.2. □

The trajectories of the system (2.3) subject to initial conditions $x(0) = x_0$ and $x'(0) = 0$ and the corresponding solution curves with physical parameters $w = 1$, $m = k = \frac{\epsilon}{\pi}$ and $V = 1$ are shown in Fig. 3. Note that x_0 is confined by $x_0 < 1$ in above Lemma, however, it is of physical interest only when $x_0 \in (0, 1)$. So the solution curves with $x_0 < 0$ lost their physical meaning, for instance, the solution curve determined by $x_0 = -0.3$ only makes mathematical sense. So we have to do more detailed analysis on x_t.

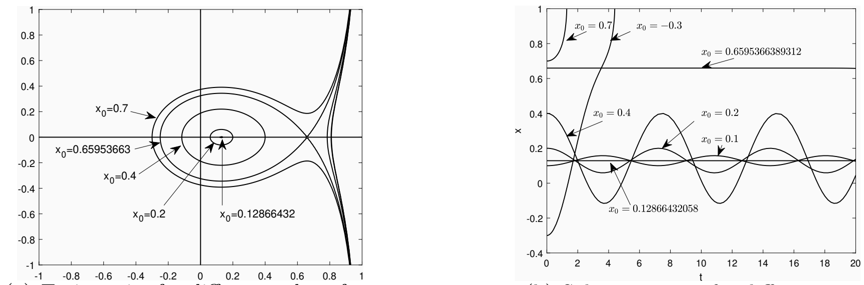

(a) Trajectories for different value of x_0 (b) Solution curves for different x_0

Figure 3. Phase portrait and corresponding solution curves with physical parameters $w = 1$, $m = k = \frac{\epsilon}{\pi}$ and $V = 1$.

Lemma 2.4. *For x_t determined by the equation* (2.8)*, there exists a critical volatge $V_c \in (0, V^*)$ such that $x_t < 0$ when $0 < V < V_c$; $x_t = 0$ when $V = V_c$; and $x_t > 0$ when $V_c < V < V^*$.*

Proof. For the case when $0 < V < V^*$, the system (2.3) has a saddle $(x_2, 0)$, where $x_2 = x_2(V)$ is determined implicitly by (see the discussion below (2.6))

$$g(x_2) = -\beta x_2(1 - x_2)^2 + B(1 - x_2)V^2 + AV^2 = 0. \tag{2.9}$$

Let $F(V) = H(x_2, 0) - H(0, 0)$ for $0 < V < V^*$, namely,

$$\begin{aligned} F(V) &= \frac{\beta}{2}x_2^2 - \frac{A}{1 - x_2}V^2 + B\ln(1 - x_2)V^2 + AV^2 \\ &= \frac{\beta}{2}x_2^2 + \ln(1 - x_2)BV^2 - \frac{x_2}{1 - x_2}AV^2. \end{aligned} \tag{2.10}$$

It follows from the equation (2.9) that

$$\frac{dx_2}{dV} = -\frac{2V\big(B(1 - x_2) + A\big)}{-3\beta x_2^2 + 4\beta x_2 - BV^2 - \beta}. \tag{2.11}$$

Note that $2V\big(B(1 - x_2) + A\big) > 0$ and $-3\beta x_2^2 + 4\beta x_2 - BV^2 - \beta > 0$ since $\frac{1}{3} < x_- < x_2 < x_+ < 1$ for $0 < V < V^*$. One has $\frac{dx_2}{dV} < 0$.

Direct calculation gives

$$F'(V) = -\frac{g(x_2)}{(1 - x_2)^2}x_2' - \frac{2A}{1 - x_2}V + 2AV = -\frac{2AVx_2}{1 - x_2} < 0, \tag{2.12}$$

which indicates that $F(V)$ is decreasing in V on $(0, V^*)$.

Recall that $x_- < x_2 < x_+$. It is easy to see that $\lim\limits_{V \to 0^+} x_- = \frac{1}{3}$. From the equation (2.9), we have $\lim\limits_{V \to 0^+} x_2(V) = 1$. And hence $\lim\limits_{V \to 0^+} F(V) = \dfrac{\beta}{2} > 0$.

Note that for $V = V^*$, $x_2(V^*)$ is an equilibrium point with multiplicity two. One has $g(x_2(V^*)) = 0$ and $g'(x_2(V^*)) = 0$. It follows from (2.5) and (2.6) that

$$\begin{aligned} &- 3\beta x_2^2 + 4\beta x_2 - \beta - B{V^*}^2 = 0, \\ &- \beta x_2(1 - x_2)^2 + B(1 - x_2){V^*}^2 + A{V^*}^2 = 0, \end{aligned}$$

which gives

$$BV^{*2} = \beta(1-x_2)(3x_2-1) \quad \text{and} \quad AV^{*2} = \beta(1-x_2)^2(1-2x_2).$$

Therefore,

$$\lim_{V\to V^{*-}} F(V) = \frac{\beta}{2}x_2(-4x_2^2+5x_2-2) + \beta(1-x_2)(3x_2-1)\ln(1-x_2) < 0 \quad (2.13)$$

since $x_2 = x_2(V^*) = \frac{2}{3} - \frac{1}{3}\sqrt{1-\frac{3BV^{*2}}{\beta}} > \frac{1}{3}$.

By the Intermediate Value Theorem for $F(V)$ and the fact that $F(V)$ is decreasing on $(0, V^*)$, there is a unique $V_c \in (0, V^*)$ such that $F(V_c) = 0$, $F(V) > 0$ for $0 < V < V_c$ and $F(V) < 0$ for $V_c < V < V^*$. It follows that $H(x_2, 0) = H(0, 0)$ at $V = V_c$, and hence $x_t = 0$; $H(x_2, 0) > H(0, 0)$ for $0 < V < V_c$, and hence $x_t < 0$; and $H(x_2, 0) < H(0, 0)$ for $V_c < V < V^*$, and hence $x_t > 0$. □

We comment that it is of physical interest only for $0 \leq x_0 < 1$. Correspondingly, in our following discussion, we further assume that $0 \leq x_0 < 1$. From Lemma 2.3 and Lemma 2.4, one has

Theorem 2.1. *For the equation* (1.4) *subject to the initial conditions* $x(0) = x_0$ $(0 \leq x_0 < 1)$ *and* $x'(0) = 0$*, together with the critical voltages* V^* *identified in* (2.7) *and* V_c *identified in Lemma 2.4, one has*

(i) *For* $V > V^*$*, it has a break solution for arbitrary* x_0*.*

(ii) *For* $V = V^*$*, it has a break solution provided that* $x_0 \neq x_2$*, however, it has a constant solution* $x = x_0$ *if* $x_0 = x_2 = \frac{2}{3} - \frac{1}{3}\sqrt{1-\frac{3B}{\beta}V^{*2}}$*.*

(iii) *For* $V_c < V < V^*$*,*

- (iii1) *when* $x_0 > x_2$ *or* $0 < x_0 < x_t$*, it has a break solution.*
- (iii2) *when* $x_0 = x_c$ *or* $x_0 = x_2$*, it has a constant solution.*
- (iii3) *when* $x_t < x_0 < x_2$*, it has a periodic solution.*
- (iii4) *when* $x_0 = x_t$*, it has a solution approaching* x_2 *as* t *goes to infinity.*

(iv) *For* $V = V_c$*,*

- (iv1) *when* $x_0 > x_2$*, it has a break solution.*
- (iv2) *when* $x_0 = x_c$ *or* $x_0 = x_2$*, it has a constant solution.*
- (iv3) *when* $0 < x_0 < x_2$*, it has a periodic solution.*
- (iv4) *when* $x_0 = 0$*, it has a solution approaching* x_2 *as* t *goes to infinity.*

(v) *For* $0 < V < V_c$*,*

- (v1) *when* $x_0 > x_2$*, it has a break solution.*
- (v2) *when* $x_0 = x_c$ *or* $x_0 = x_2$*, it has a constant solution.*
- (v3) *when* $0 \leq x_0 < x_2$*, it has a periodic solution.*

The trajectories of the system (1.4) and its corresponding solution curves with different values of V for fixed $w = 1$ and $m = k = \frac{\epsilon}{\pi}$ and $x_0 = 0$ are shown in Figure 3, which provides more intuitive illustration of our analytical results.

To end this section, we remark that the identification of the critical voltages V^* and V_c are crucial in our analysis, and their roles played in our study are characterized in details. This provides better understanding of the dynamics of

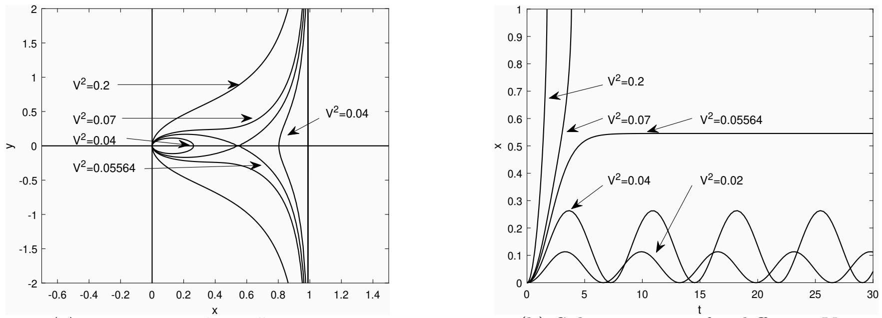

(a) Trajectories for different V (b) Solution curves for different V

Figure 4. Trajectories and corresponding solution curves with $x_0 = 0$ and $w = 1$ and $m = k = \frac{\epsilon}{\pi}$. Under the specific setup, one has $V_c = 0.4180909$ and $V^* = 0.6764614$. We also point out that once the value of V is fixed, the corresponding values for x_2, x_c and x_t can be uniquely determined.

the MEMS, particularly the pull-in instability phenomena. Meanwhile, it provides efficient ways to control the voltage applied to the system to avoid the pull-in instability phenomena. We would also like to point out that the results obtained in this section are based on rigorous mathematical analysis and non-intuitive.

3. Pull-in instability for MEMS

For a given MEMS, the motion of the plate caused by voltage is nonlinear, which is further illustrated by Theorem 2.1, particularly, the dependence of the dynamical behaviors of the moving plate on both the voltage and the initial position. To further illustrate our mathematical results from the point of more physical review, we establish the following result in terms of the terminology pull-in instability.

Theorem 3.1. *For a parallel-plate electrostatic MEMS actuator, suppose that the position of the fixed plate is at $x = 1$, and the initial position of the movable plate is at $x = x_0$ with $0 \leq x_0 < 1$, and the initial speed is zero. Then, there exist two critical voltages V_c and V^* with $0 < V_c < V^*$ and V^* being determined by* (2.7) *such that*

(i) *If $V > V^*$, independent of the initial position, the pull-in occurs.*

(ii) *If $V = V^*$, the movable plate remains static for $x_0 = x_2$, while pull-in occurs for any other x_0.*

(iii) *If $V_c \leq V < V^*$, the movable plate oscillates periodically for $x_t < x_0 < x_2$; the pull-in occurs for either $x_2 < x_0 < 1$ or $0 < x_0 < x_t$; the movable plate remains static for either $x_0 = x_1$ or $x_0 = x_2$; while the movable plate approaches the equilibrium position slowly as $t \to \infty$ for $x_0 = x_t$.*

(iv) *If $0 < V < V_c$, the movable plate oscillates periodically for $0 \leq x_0 < x_2$; the pull-in occurs for $x_2 < x_0 < 1$; while the movable plate remains static for either $x_0 = x_1$ or $x_0 = x_2$.*

We comment that so far we mainly focus on the study of the effects from the voltage and initial positions while other system parameters are fixed. To better understand the system, particularly, the critical roles played by the system parameters involved in the system, we next conduct some numerical experiments examining the effects from other system parameters w, k and m, respectively for fixed ϵ and voltage V (see Figure 5).

Taking the most left figure in Figure 5 for example, one observes that there exists a unique critical value w^* for fixed other system parameters such that for $w > w^*$, the pull-in phenomenon occurs. furthermore, for $w < w^*$, the amplitude of the solution increases in w. Similar phenomena are observed for the parameters k and m from the middle figure and the most right one in Figure 5, respectively.

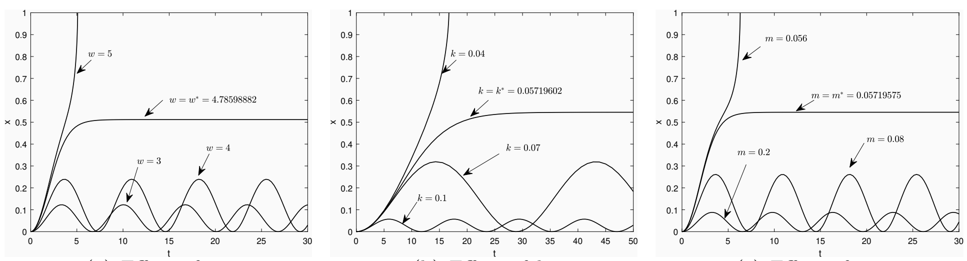

(a) Effect of w (b) Effect of k (c) Effect of m

Figure 5. The solution curves of the equation 1.4 with $\epsilon = 1$ and $V = 0.1$ for different setups: (a) $m = 1$ and $k = 1$, (b) $m = 1$ and $w = 1$, (c) $w = 1$ and $k = 1$.

4. Acknowledgment

We would like to thank Prof Jihuan He from Suchow University for introducing such an interesting research project and valuable suggestions to further improve the manuscript.

5. Concluding remarks

In this work, we analyze typical electrostatic MEMS actuators via dynamical system approach. Critical voltages are identified, and they splits the voltage range into different subranges, over which distinct and rich dynamics of the system are observed, particularly, the pull-in in stability phenomena are characterized further depending on the nonlinear interplays among other system parameters. The effects from different system parameters are examined both analytically (such as the voltage and initial positions) and numerically (such as the parameters w, k and m). The detailed analysis provides some efficient ways to control the dynamical behavior of the system so that one is able to avoid the occurrence of the pull-in instability. Together, this provides better understanding of the system and could stimulate further studies of related topics.

References

[1] S. Ai and J. A. Pelesko, *Dynamics of a canonical electrostatic MEMS/NEMS system*, Journal of Dynamics and differential Equations, 2008, 20(3), 609–641.

[2] N. Anjum and J. He, *Nonlinear dynamic analysis of vibratory behavior of a graphene nano/microelectromechanical system*, Mathematical Methods in the Applied Sciences, 2020, DOI: 10.1002/mma.6699.

[3] O. Akar, T. Akin and K. Najafi, *A wireless batch sealed absolute capacitive pressure sensor*, Sensors & Actuators A Physical, 2001, 95(1), 29–38.

[4] D. Elata and H. Bamberger, *On the dynamic pull-in of electrostatic actuators with multiple degrees of freedom and multiple voltage sources*, Journal of Microelectromechanical Systems, 2006, 15(1), 131–140.

[5] M. Gomez, D. E. Moulton and D. Vella, *Delayed pull-in transitions in overdamped MEMS devices*, Journal of Micromechanics and Microengineering, 2018, 28, 015006.

[6] J. He, N. Qie, C. He, et al., *Fast identification of the pull-in voltage of a nano/micro-electromechanical system*, Journal of Low Frequency Noise, Vibration and Active Control, 2022, 0(0), 1–6.

[7] L. Jang, W. Kan, M. Chen, et al., *Parameter extraction from BVD electrical model of PZT actuator of micropumps using time-domain measurement technique*, Microfluidics and Nanofluidics, 2009, 7, 559–568.

[8] J. Li, *Geometric Properties and Exact Travelling Wave Solutions for the Generalized Burger-Fisher Equation and the Sharma-Tasso-Olver Equation*, Journal of Nonlinear Modeling and Analysis, 2019, 1(1), 1–10.

[9] C. Liu and Y. Yan, *Resonances and chaos of electrostatically actuated arch micro/nanoresonators with time delay velocity feedback*, Chaos Solitons & Fractals, 2019, 131, 109512.

[10] G. Michael, V. Dominic and M. Derek, *Pull-in dynamics of overdamped microbeams*, Journal of Micromechanics and Microengineering, 2018, 28, 115002.

[11] C. T. C. Nguyen, L. P. B. Katehi and G. M. Rebeiz, *Micromachined devices for wireless communications*, Proceedings of the IEEE, 1998, 86, 1756–1768.

[12] A. H. Nayfeh, M. I. Younis and E. M. Abdel-Rahman, *Dynamic pull-in phenomenon in MEMS resonators*, Nonlinear Dynamics, 2007, 48(1–2), 153–163.

[13] Y. Nemirovsky and O. Bochobza-Degani, *A Methodology and Model for the Pull-In Parameters of Electrostatic Actuators*, Journal of Microelectromechanical Systems, 2001, 10(4), 601–614.

[14] H. C. Nathanson, W. E. Newell, R. A. Wickstrom, et al., *The resonant gate transistor*, IEEE Transactions on Electron Devices, 1967, 14(3), 117–133.

[15] G. H. Nielson and G. Barbastathis, *Dynamic pull-in of parallel-plate and torsional electrostatic MEMS actuators*, Journal of Microelectromechanical Systems, 2006, 15(4), 811–821.

[16] H. M. Ouakad, *Nonlinear structural behavior of a size-dependent MEMS gyroscope assuming a non-trivial shaped proof mass*, Microsystem Technologies, 2019, 26(6), 573–582.

[17] H. B. Palmer, *The Capacitance of a Parallel-Plate Capacitor by the Schwartz-Christoffel Transformation*, American Institute of Electrical Engineers Transactions of Electrical Engineers, 1937, 56(3), 363–366.

[18] H. Shang, *Pull-in instability of a typical electrostatic MEMS resonator and its control by delayed feedback*, Nonlinear Dynamics, 2017, 90, 171–183.

[19] S. Schonhardt, J. G. Korvink, J. Mohr, et al., *Optimization of an electromagnetic comb drive actuator*, Sensors & Actuators A Physical, 2009, 154(2), 212–217.

[20] H. M. Sedighi, M. Changizian and A. Noghrehabadi, *Dynamic pull-in instability of geometrically nonlinear actuated micro-beams based on the modified couple stress theory*, Latin American Journal of Solids and Structures, 2014, 11(5), 810–825.

[21] H. A. C. Tilmans, R. Legtenberg, H. Schurer, et al., *(Electro-) mechanical characteristics of electrostatically driven vacuum encapsulated polysilicon resonators*, IEEE Transactions on Ultrasonics Ferroelectrics & Frequency Control, 1994, 41, 4–6.

[22] F. Tajaddodianfar, M. Yazdi and H. N. Pishkenari, *Nonlinear dynamics of MEMS/NEMS resonators: analytical solution by the homotopy analysis method*, Microsystem Technologies, 2017, 03, 1–14.

[23] D. Tian, Q. T. Ain and N. Anjum, *Fractal N/MEMS: from pull-in instability to pull-in stability*, Fractals, 2020, 29(2), 2150030.

[24] M. I. Younis, *MEMS linear and nonlinear statics and dynamics*, Springer, New York, 2011.

[25] L. Zhang, Y. Wang, C. M. Khalique, et al., *Peakon and cuspon solutions of a generalized Camassa-Holm-Novikov equation*, Journal of Applied Analysis and Computations, 2018, 8(6), 1938–1958.